Theoretical study of the gas-phase thermolysis of 3-methyl-1,2,4,5-tetroxane

ARTICLE *in* JOURNAL OF MOLECULAR MODELING · JUNE 2014

Impact Factor: 1.74 · DOI: 10.1007/s00894-014-2224-6 · Source: PubMed

J Mol Model (2014) 20:2224
DOI 10.1007/s00894-014-2224-6

ORIGINAL PAPER

Theoretical study of the gas-phase thermolysis of 3-methyl-1,2,4,5-tetroxane

Mariela Inés Profeta · Jorge Marcelo Romero · Nelly Lidia Jorge · André Grand · Alfonso Hernández-Laguna

Received: 2 December 2013 / Accepted: 23 March 2014

Abstract Cyclic organic peroxides are a broad and highly sought-after class of peroxide compounds that present high reactivity and even explosive character. The unusually high reactivity of these peroxides can generally be attributed to the rupture of O–O bonds. Cyclic diperoxides are a very interesting series of substituted compounds in which tetroxane is the most prominent member. Gas-phase thermolysis of the simplest substituted member of the series [3-methyl-1,2,4,5-tetroxane or methylformaldehyde diperoxide (MFDP)] has been observed to yield one acetaldehyde, one formaldehyde, and one oxygen molecule as reaction products. DFT at the 6-311+G** level of theory using the BHANDHLYP correlation–exchange functional was applied via the Gaussian09 program to calculate the critical points of the potential energy surface (PES) of this reaction. Equatorial and axial isomers were studied. The singlet state PES of MFDP was calculated, and an open diradical structure was found to be the first intermediate in a stepwise reaction. Two PESs were subsequently obtained: singlet state (S) and triplet state (T) PESs. After that, two alternative stepwise reactions were found to be possible: 1) one in which either an acetaldehyde, or 2) formaldehyde molecule is initially formed. For second one, exothermic reactions were observed for both the S and T PESs. The reaction products include a oxygen molecule in either S or T state, with the T reaction being the most exothermic. When calculations were performed at the CASSCF(10,10)/6-311+G** level, spin–orbit coupling permitted S to T crossing at the open diradical intermediate stage, a non-adiabatic reaction was observed, and lower activation energies and higher exothermicity were generally seen for the T PES than for the S PES. These results were compared with the corresponding results for tetroxane. The spin–orbit coupling of MFDP and tetroxane yielded identical values, so it appears that the methyl substituent does not have any effect on this coupling.

Keywords Cyclic diperoxides · 3-Methyl-1,2,4,5-tetroxane/methylformaldehyde diperoxide · Gas-phase thermolysis reaction · DFT · Potential energy surface · Equatorial and axial isomers · Reaction mechanisms

This paper belongs to Topical Collection QUITEL 2013

Electronic supplementary material The online version of this article (doi:10.1007/s00894-014-2224-6) contains supplementary material, which is available to authorized users.

M. I. Profeta · J. M. Romero · N. L. Jorge
Área de Química Física, Facultad de Ciencias Exactas y Naturales y Agrimensura, UNNE, Avda. Libertad 5460, 3400 Corrientes, Argentina

A. Grand
INAC, SCIB, Laboratoire "Lésions des Acides Nucleiques", UMR CEA-UJF E3, CEA-Grenoble, 17 Rue des Martyrs, 38054 Grenoble Cedex 9, France

A. Grand
Universidad Autónoma de Chile, Carlos Antúnez 1920, Providencia, Santiago, Chile

A. Hernández-Laguna (✉)
Instituto Andaluz de Ciencias de la Tierra (UGR-CSIC), Avda. de las Palmeras 4, 18100 Armilla, Granada, Spain
e-mail: alfonso.hernandez@iact.ugr-csic.es

Introduction

Organic peroxides are a broad and highly sought-after class of organic compounds [1–4] that present many interesting capabilities, including high reactivity and even explosive reactions. These unusually high reactivities of peroxides can be generally attributed to the rupture of O–O bonds.

These compounds have found wide application in industrial and laboratory synthesis as oxidants, polymerization initiators, crosslinking agents, and explosive compounds, and some have

Published online: 22 May 2014

been found to have antimalarial and antimicrobial activities [5–7].

The thermal decomposition of 1,2,4,5-tetroxanes has already received considerable attention [8–10]. Most recently, accurate experimental investigations on simple substituted tetroxanes have provided coherent information on their activation parameters. The reaction yield has been studied as a function of the degree and pattern of substitution [11–14]. Steric, inductive, mesomeric, and stereoelectronic effects of different substituents on the peroxidic bond strength should also be considered, as the scission of this bond is the driving step in the initial unimolecular gas-phase thermolysis. Effects of the solvent may also be relevant to the reactivities of these compounds. Using all of the resulting data, reaction mechanisms can be proposed and new substituted compounds can be formulated.

In a previous paper, the gas-phase thermolysis of formaldehyde diperoxide (1,2,4,5-tetroxane), the simplest derivative of the series, was studied theoretically [15]. Thermolysis of this compound yields two molecules of formaldehyde and one of oxygen, and—despite the simplicity of the reaction products—the reaction was found to be very complex because the paths on the potential energy surface (PES) of the ground singlet state (S) must be treated with balanced accuracy and, since nonadiabatic surface crossing is involved, the first triplet state (T) must also be determined. Therefore, in addition to the locations of critical points on the PESs for the ground and excited states, characterizing the regions where both surfaces intersect is of great interest. Furthermore, two mechanisms are possible: (i) a stepwise unimolecular homolytic mechanism, and (ii) a concerted mechanism where bond creation and bond breaking can occur simultaneously. In our previous paper, we investigated the concerted mechanism for the thermolysis of the tetroxane, and found that it had a much higher activation energy than the stepwise mechanism [15].

Based on that initial theoretical study [15], the following mechanism for the gas-phase thermolysis of tetroxane was proposed. Tetroxane decomposition is initiated in the singlet state by O–O bond homolysis, and then the decomposition can proceed by either of two different pathways, either (i) on the S PES or (ii) on the T PES. If the first surface is followed, then two molecules of formaldehyde and one S oxygen molecule are produced and an endothermic reaction occurs. However, if the reaction is on the T PES, a nonadiabatic crossing from the S to the T surface takes place, two formaldehyde molecules and one oxygen molecule in the ground T are obtained, and an exothermic reaction transpires [15]. The latter mechanism is much more in agreement with the known experimental reactivity of this compound, and similar mechanisms have been found for the thermal decomposition of 1,2-dioxetane [16–18]. Besides, in the gas-phase thermolysis of 3,3,6,6-tetramethyl-1,2,4,5-tetroxane, luminescence was observed at 435 nm, which indicates that an excited electronic state is involved in the reaction [19].

Various substituted tetroxanes have been studied in depth using a variety of experimental and theoretical techniques [11–14, 20–24]; however, to our knowledge, the mechanism for the nonadiabatic crossing between the S and T surfaces has not been studied as a function of the substituent yet. Therefore, in the work reported in the present paper, we studied the mechanism for the gas-phase thermolysis of the simplest substituted member [3-methyl-1,2,4,5-tetroxane, methylformaldehyde diperoxide (MFDP)] of this series of compounds, using several high-level computational methods. The S and T PESs, the possible S/T crossing regions, and the spin–orbit coupling of MFDP were also investigated theoretically in order to predict the efficiency of intersystem crossing.

Computational methods

The calculations were performed using DFT with the 6-311+G** basis set and the BHANDHLYP [25–27] correlation–exchange functional. The critical points on the PESs of the ground S and first T of the reaction were determined. The critical points on the PESs were explored and located using a stepwise procedure: first, DFT was applied at the 3-21+G** level to prospect for critical points along the hypothetical reaction pathways on the S and T PESs; then, the 6-311+G** basis set was used for reoptimize the critical points on the PESs found at the previous level. Calculations were performed with the Gaussian 09 program [28]. Critical points on the PESs were optimized by the Berny method [29], and transition states were located with aid of the eigenvalue following method [30]. Minima and transition states were characterized by studying their harmonic vibrational frequencies (minima had all frequencies positive and transition states had only one imaginary frequency). Transition vectors (a transition vector is the normal coordinate of the imaginary frequency of a transition state, TS) were depicted using the GaussView program [31]. Transition vectors were drawn as arrows between the atoms of the transition structures of the reaction profiles. The total energy plus ZPE was used to calculate relative energies. The IRC method [32, 33] was used to determine how the TSs are linked to their reactants and products. The are two isomers of MFDP according to whether the methyl group is located at the axial or equatorial position on the cyclic diperoxide ring. It is generally assumed that the two isomers of MFDP decompose and react to yield diradical intermediates. These intermediates are formed following the initial cleavage of one of the O–O bonds [11–14, 20–24]. The CASSCF(10,10)/6-311+G** level of theory [34–37] was used to calculate the spin–orbit couplings [29, 30, 38, 39] at the open diradical critical points on both the S and T PESs. The active space is similar to that described in [15].

Results and discussion

Reaction pathways in the S PES

Scheme 1 shows two hypothetical reaction pathways (S-I and S-II) for the gas-phase thermolysis of MFDP. These reaction pathways yield one molecule of formaldehyde, one molecule of acetaldehyde, and molecular oxygen as final products.

Pathway S-I

In this pathway, the reactant has a closed cyclic diperoxide ring in a chair conformation (**S-c** in Scheme 1). The equatorial isomer is 3.2 kcal/mol more stable than the axial isomer. An interchange between the isomers can occur.

Scission of one of the peroxidic bonds in equatorial **S-c** leads to a diradical (O↓···↑O, **S-o**) open intermediate via **S-TSco** (Figs. 1 and 2; reaction profiles for the axial isomer are found in the "Electronic supplementary material," ESM). The activation energies are 17.1 and 16.4 kcal/mol for the equatorial and axial isomers, respectively (Table 1a and b, respectively). Thus, the presence of the methyl in the equatorial position slightly stabilizes the peroxidic bond, meaning that a larger activation energy is required to break it. The O···O bond distance in this S-TS (Fig. 1) is 1.924 or 1.903 Å for the equatorial or axial isomer, respectively. The transition vector is mainly related to the opening of the O–O bond. In this structure, the spin density is close to ±0.8 on the open oxygens, indicating the diradical singlet state character of this TS. **S-TSco** leads to the **S-o** intermediate, which is 11.4 kcal/mol (for the equatorial isomer) or 9.3 kcal/mol (for the axial isomer) less stable than the **S-c** respective isomer.

The open equatorial isomer intermediate **S-o** (Fig. 1) presents an O↓···↑O distance of 3.47 Å and a dihedral angle (O–C–O–O) of 73.2°. It is considered to have *gauche* and *syn* conformations of the two C–O bonds, in agreement with those of tetroxane [15]. The open axial isomer intermediate **S-o** (Fig. S1 of the ESM) presents an O↓···↑O distance of 3.42 Å and a dihedral angle (O–C–O–O) of 73.5°. It is considered to have *gauche* and *anti* conformations of the two C–O bonds. The O↓···↑O distance is larger in tetroxane (3.52 Å [15]) than in MFDP. The axial **S-o** isomer has a shorter O↓···↑O distance and a smaller endothermic energy than the equatorial isomer. The spin densities of both of the radical Os are close to ±1, showing the clear diradical character of both open structures. The shortest bond distances and angles in **S-TSco** and **S-o** correspond to the lowest activation and reaction energies of the axial isomer, in agreement with the Leffler–Hammond principle [40, 41]. The equatorial isomer has the largest activation energy for the dissociation of the most reactive peroxidic bond, and reaches a slightly more stable **S-o** intermediate than the axial isomer does.

After this initial step, the thermolytic reaction branches and continues along one of two different stepwise pathways (Scheme 1), as described below

Pathway S-Ia. The first step occurs with the scission of the H_2C–O bond in **S-o** to give one molecule of formaldehyde and an S peroxyacetaldehyde open diradical, **S-b′** (Scheme 1, Fig. 1, Table 1), which is 7.1/4.8 kcal/mol less stable than **S-c** (equatorial or axial). This step occurs via **S-TSob′** (Fig. 1 and Table 1a and b for the equatorial and axial isomers, respectively), which is generated when the C–OOC(CH_3)O bond is broken. This requires approximately the same activation energy (20.7/20.8 kcal/mol) and leads to a C···OO bond distance of 1.72 Å for both isomers. From this point on, we ignore the supermolecular complex with formaldehyde and the peroxyacetaldehyde diradical, and consider only the diradical structure (**S-b**, Fig. 3). In a second step, the other C–O bond in the peroxyacetaldehyde diradical is cleaved to yield molecular oxygen and an acetaldehyde molecule, **S-p** (Scheme 1, Fig. 3), both of which are in the singlet state. This product is exothermic by −28.6/−29.0 kcal/mol (equatorial/axial isomer) with respect to the previous step in the reaction mechanism. This product is generated via **S-TSbp**, which has an activation energy of 11.4/11.7 kcal/mol.

Pathway S-Ib. This reaction pathway is very similar to the previous one, with the exception that the first molecule after the first step is an acetaldehyde instead of a formaldehyde. Thus, the first step involves the scission of a CH_3C–O bond in **S-o** to give one molecule of acetaldehyde and a singlet state peroxyformaldehyde open diradical, **S-b″** (Scheme 1, Fig. 2). In the second step, involving only the peroxyformaldehyde diradical, the other C–O bond of the peroxyformaldehyde radical is cleaved to yield molecular oxygen and a formaldehyde molecule, **S-p′** (Scheme 1, Fig. 4), with an endothermicity of 5.7 kcal/mol.

The first step involves a transition structure, **S-TSob″** (Fig. 2 and Table 2a, b for the equatorial and axial isomers, respectively), generated when the C–OO bond is broken, which leads to a C···OO bond distance of 1.72 Å for both isomers (similar to the equivalent distance found for **S-TSob′**). The activation energy is 17.9/15.5 kcal/mol (equatorial/axial isomer; Fig. 2, Table 2). The second step also involves a transition structure, **S-TSb″′p′**, and the activation energy for this is 13.9 kcal/mol (Fig. 4).

In pathway S-Ib, the activation energies for the formation of acetaldehyde and peroxyformaldehyde diradical (**S-o** → **S-b″**) are lower and there are larger differences between the TSs generated from the equatorial and axial isomers than seen in the formation of formaldehyde and peroxyacetaldehyde diradical (S-Ia, **S-o** → **S-b′**). In this study, the stability trends for the MFDP can be rationalized by invoking the effect of repulsive interactions of the methyl

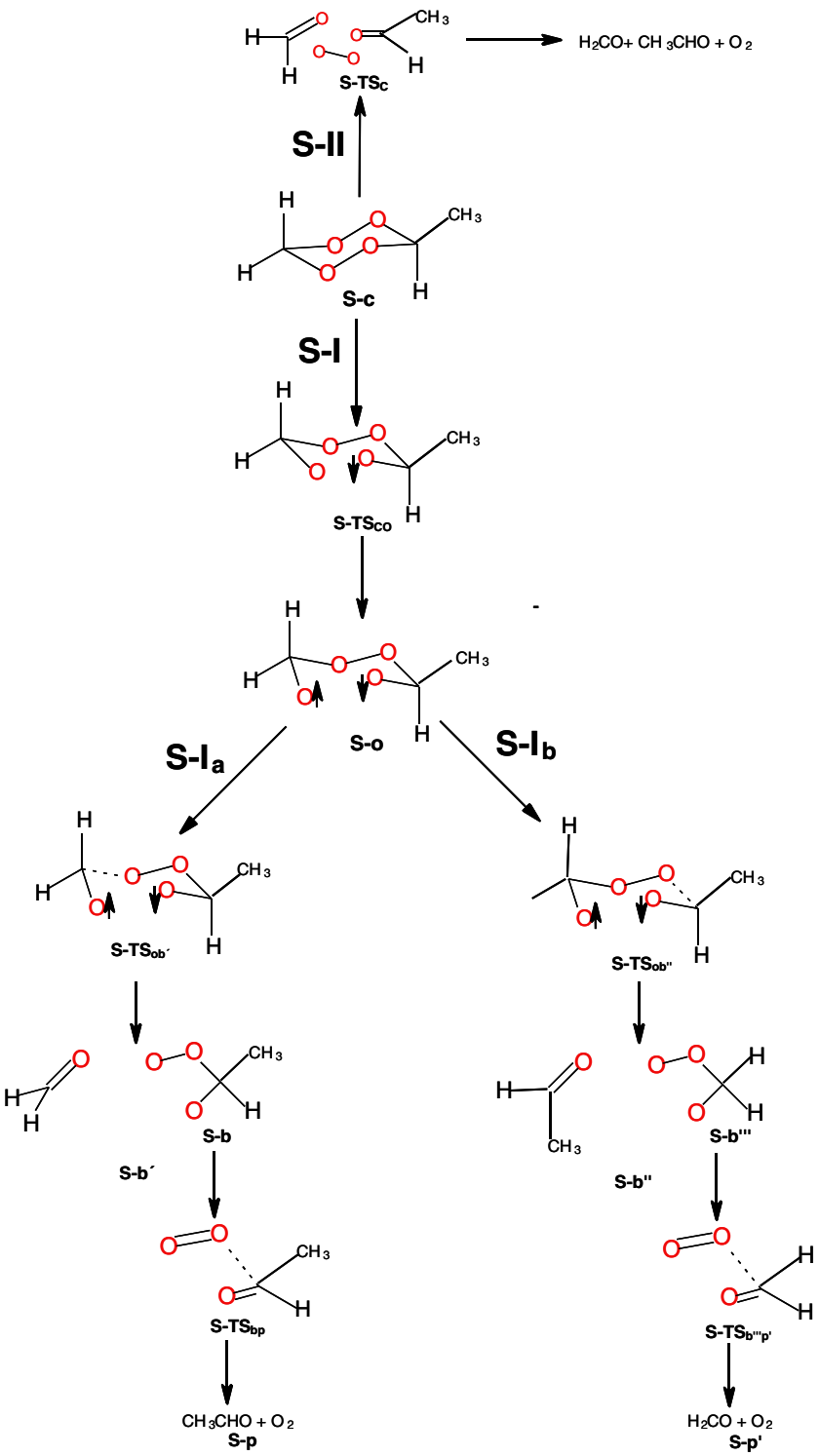

Scheme 1 Hypothetical reaction pathways for the S state in the thermolysis of MFDP. S-I is the stepwise mechanism and S-II is the concerted mechanism

substituent on the O–O and C–O bonds in the peroxide ring, which in turn decreases the activation energy for the formation of acetaldehyde and peroxyformaldehyde diradical. Besides, the equatorial/axial effect is more conspicuous for **S-TSob″** than it is for **S-TSob′**, due to the proximity of the methyl group to the reactive bond.

The exothermicity of the reaction (−28.0/−29.0 kcal/mol for the equatorial/axial isomers) for pathway S-Ia is in good agreement with the known reactivities of these compounds, and the activation energies obtained. The first step of pathway S-Ia (20.7 kcal/mol) is the rate-limiting step of the reaction. However, if the reaction proceeds via pathway S-Ib, the rate

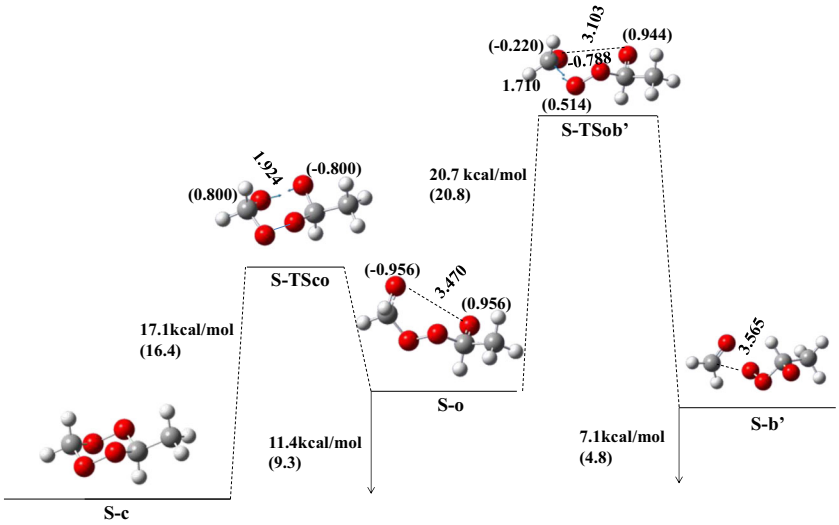

Fig. 1 Reaction profile of pathway S-Ia in Scheme 1. For each structure, the energies (in kcal/mol) of the equatorial isomer (*not in parentheses*) and the axial isomer (*in parentheses*) are displayed. Activation energies were calculated from **S-c** or **S-o**. Bond lengths (in Å) are shown next to the respective bonds. Spin densities are shown *next to the respective atoms in parentheses*. *White, gray, and red spheres* indicate hydrogen, carbon, and oxygen atoms, respectively. The full axial isomer reaction profile is given in the ESM

limiting step is **TSob″** in the equatorial isomer, however the activation energy is very similar to TSco, but in the axial isomer the rate limiting step is **TSco**.

Pathway S-II

Products are generated from compound **S-c** in a one-step concerted mechanism via a transition state (**S-TSc**) with an activation energy of 72.9 kcal/mol for the equatorial isomer and 70.2 kcal/mol for the axial isomer (Table 3, Fig. 5). This mechanism is exothermic (21.4 and 4.2 kcal/mol for the equatorial and axial isomers, respectively) and has been proposed hypothetically [8–10] but has never been explicitly tested. Considering the high activation energy for this pathway, it is unlikely to occur.

Comparison with tetroxane

If we compare the reaction profile of methyltetroxane with that of tetroxane [15], similar activation energies are seen for the first reaction step in the S-I pathway, **S-c→S-o**, and the methyltetroxane reaction involves a slightly more stable open **S-o** structure. However, for the **S-o→S-b′** and **S-b→S-p** steps in pathway S-Ia, the activation energies for MFDP are lower than those for tetroxane. On the other hand, for the S-Ib pathway, the steps **S-b″→S-p′** show the same products and the same heats of reaction for both MFDP and tetroxane. In the last step of the S-Ia pathway, **S-b→S-p** is exothermic for MFDP but endothermic for tetroxane. These facts

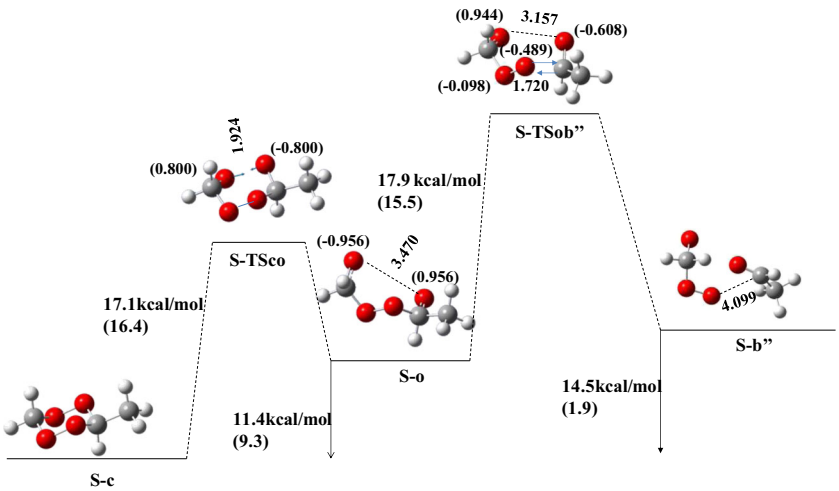

Fig. 2 Reaction profile of pathway S-Ib in Scheme 1. For each structure, the energies (in kcal/mol) of the equatorial isomer (*not in parentheses*) and the axial isomer (*in parentheses*) are displayed. Activation energies were calculated from **S-c** or **S-o**. Bond lengths (in Å) are shown next to the respective bonds. Spin densities are shown *next to the respective atoms in parentheses*. *White, gray, and red spheres* refer to hydrogen, carbon, and oxygen atoms, respectively. The full axial isomer reaction profile is given in the ESM

Table 1 Total energies (E),[a] zero-point energies (ZPE),[a] imaginary frequencies (ν),[b], spin contamination (S^2), and relative energies (ΔE),[c] of critical points on the singlet ground-state PES in the thermolysis of 3-methyl-1,2,4,5-tetroxane via the S-Ia pathway. Values for (a) equatorial isomers and (b) axial isomers are shown separately

Structure	E[a]	ZPE[a]	ν[b]	(S^2)	ΔE[c]
(a)					
S-c	−418.51964	0.10414		0.00	0.00
S-TSco	−418.488059	0.09984	298	0.027	17.11
S-o	−418.49492	0.09759		0.081	11.46
S-TSob′	−418.45957	0.09542	908	0.469	32.22 (20.75)[d]
S-b′	−418.49793	0.09376		0.099	7.10
S-b	−304.01888	0.06487		0.099	0.00
S-TSbp	−303.99738	0.06156	4396	0.389	11.40
S-p	−304.061379	0.06172		0.072	−28.64
(b)					
S-c	−418.51460	0.10422		0.00	0.00
S-TSco	−418.48403	0.09985	351	0.026	16.44
S-o	−418.49319	0.09768		0.082	9.33
S-TSob′	−418.45795	0.09551	901	0.469	30.08 (20.76)[d]
S-b′	−418.49666	0.09391		0.096	4.79
S-b	−304.01829	0.06501		0.094	0.00
S-TSbp	−303.99673	0.06219	3892	0.377	11.75
S-p	−304.06126	0.06176		0.072	−29.01

[a] Energies in hartrees

[b] Imaginary frequencies in cm^{-1}

[c] Relative energies in kcal/mol, $\Delta E=[E_{total}+ZPE](c/b)-[E_{total}+ZPE](i)$ where i represents any critical point of the species in the table

[d] Relative energies in kcal/mol with respect to **S-o**

indicate why MFDP is more reactive and possibly more explosive than tetroxane. In the pathway involving a concerted mechanism (S-II), similar results were found for both compounds.

Reaction pathways for the T PES

Following previous studies in tetroxane [15], the reaction was also calculated from the first triplet state (**T-o**). Only one pathway is proposed (T-I, see Scheme 2), which is equivalent to pathway S-I. Reaction pathway T-I leads to one formaldehyde, one acetaldehyde, and one oxygen (in the ground triplet state) molecule by means of a stepwise mechanism (Scheme 2).

We found an initial triplet-state diradical open structure, **T-o**, which was very similar to the corresponding structure in the S PES, with a O↑···O↑ distance of 3.48 Å for the equatorial isomer and 3.43 Å for the axial isomer—very close to the corresponding distances for the isomers of the **S-o** state. The **T-o** and **S-o** intermediates also show very similar stabilities (ΔE=0.081 and 0.019 kcal/mol between the S and T equatorial and axial isomers, respectively, with the equatorial **S-o**

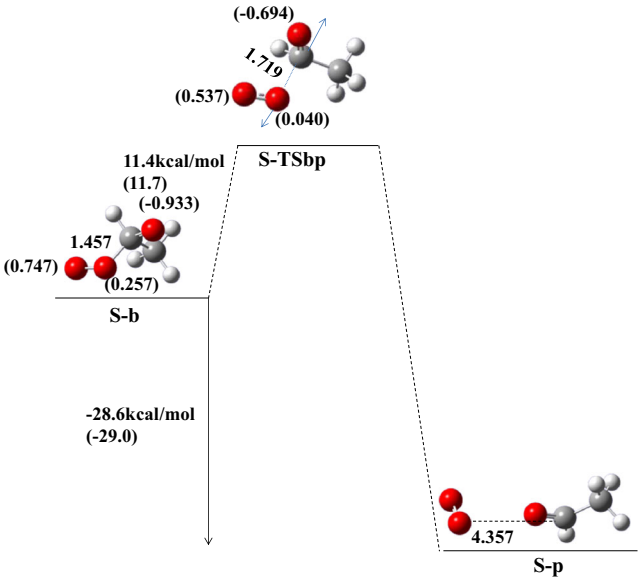

Fig. 3 Reaction profile of the second part of pathway S-Ia in Scheme 1. For each structure, the energies (in kcal/mol) of the equatorial isomer (*not in parentheses*) and the axial isomer (*in parentheses*) are displayed. Activation energies were calculated from **S-b**. Bond lengths (in Å) are shown next to the respective bonds. Spin densities are shown *next to the respective atoms in parentheses*. *White, gray, and red spheres* refer to hydrogen, carbon, and oxygen atoms, respectively. The full axial isomer reaction profile is given in the ESM

state being the most stable; see Tables 1 and 4) and have approximately the same structure. Following the methodology described in [15], given the rather similar stabilities and structures of the **S-o** intermediates in the S and T PESs, a crossing point is expected between the intermediates on both surfaces. Therefore, if spin-orbit coupling is present between both S and T surfaces, particularly between the **S-o** intermediates on those surfaces (as it is in tetroxane [15]), the reaction could proceed from this critical point from either the ground singlet state or the first triplet state surface.

Pathway T-I

Pathway T-I can follow one of two different branches after **T-o**: T-Ia and T-Ib.

Pathway T-Ia (Scheme 2). A transition state, **T-TSob′**, is generated from **T-o** (Fig. 6, Table 4a and b for the equatorial and axial isomers, respectively), which then yields a peroxyacetaldehyde diradical plus one formaldehyde molecule intermediate, **T-b′**, for both isomers. The activation energy with respect to the previous reactant is 20.6 kcal/mol for both isomers (Table 4), which is very close to that of **S-TSob′**.

From this point on, only the diradical peroxyacetaldehyde intermediate, **T-b**, will be considered. From this minimum structure, the reaction yields one T oxygen and one acetaldehyde molecule via the transition state **T-TSbp**, with an activation energy of 7.9 kcal/mol for both isomers (Fig. 7,

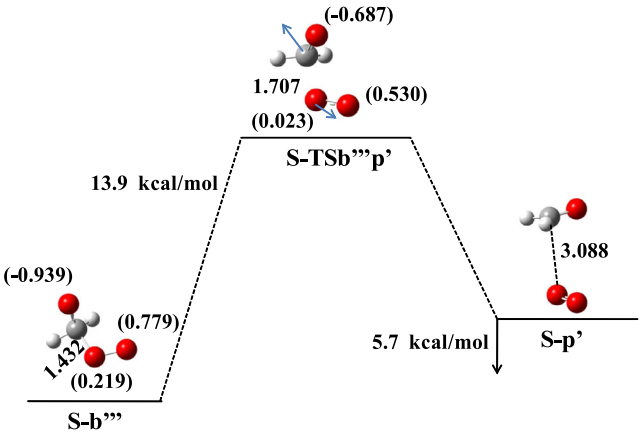

Fig. 4 Reaction profile of the second part of pathway S-Ib in Scheme 1. Energies are in kcal/mol, and bond lengths are in Å. Spin densities are shown *next to the respective atoms in parentheses*

Table 4a, b for the equatorial and axial isomers, respectively). The products of this pathway are a complex of one acetaldehyde molecule plus one T oxygen molecule, which is 40.1 kcal/mol more stable than the previous reactant.

Pathway T-Ib (Scheme 2). Here, the transition state **T-TSob″** is generated from compound **T-o** (Fig. 8, Table 5a and b for the equatorial and axial isomers, respectively). This in turn yields a peroxyformaldehyde diradical plus one acetaldehyde molecule intermediate, **T-b″**, for both isomers. The activation energy with respect to the previous reactant is 17.1 kcal/mol. This value is similar to that of the corresponding structure in the S PES (**S-TSob″**).

Table 2 Total energies (E),[a] zero-point energies (ZPE),[a] imaginary frequencies (ν),[b], spin contamination (S^2), and relative energies (ΔE),[c] of critical points on the singlet ground-state PES in the thermolysis of 3-methyl-1,2,4,5-tetroxane via the S-Ib pathway. Values for (a) equatorial isomers and (b) axial isomers are shown separately

Structure	E^a	ZPE[a]	ν^b	(S^2)	ΔE^c
(a)					
S-TSob″	−418.46386	0.09509	867	0.454	29.32 (17.86)[d]
S-b″	−418.48808	0.09565		0.099	14.48
S-b‴	−264.71320	0.03590		0.095	0.00
S-TSb‴p	−264.68812	0.03294	3950	0.417	13.88
S-p′	−264.70056	0.03233		0.000	5.69
(b)					
S-TSob″	−418.46592	0.09517	884	0.418	24.86 (15.53)[d]
S-b″	−418.50711	0.09432		0.098	1.51
S-b‴	−264.71320	0.03590		0.095	0.00
S-TSb‴p	−264.68812	0.03294	3950	0.417	13.88
S-p′	−264.70056	0.03233		0.000	5.69

[a] In hartrees

[b] Imaginary frequencies in cm^{-1}

[c] Relative energies in kcal/mol, $\Delta E=[E_{total}+ZPE](c/b''')-[E_{total}+ZPE](i)$ where i represents any critical point of the species in the table. c from Table 1

[d] Relative energies in kcal/mol with respect to **S-o**

From the minimum peroxyformaldehyde diradical intermediate, **T-b‴**, the reaction continues with the generation of one T oxygen and one formaldehyde molecule via **T-TSb‴p′**, with an activation energy of 9.6 kcal/mol regardless of the isomer considered (Fig. 9, Table 5a, b for the equatorial and axial isomers, respectively). The transition vector shows diverging arrows for the C···O distance. The products (one formaldehyde molecule plus one T oxygen molecule) are 36.3 kcal/mol more stable than the previous reactants, in agreement with the known reactivities of cyclic diperoxides.

The **T-b′** molecular complex was also similar to the equivalent structure on the S surface for both isomers, but both product complexes arising from both isomers are associated with exothermic reactions (−5.0 and −5.5 kcal/mol for the equatorial and axial isomers, respectively). Meanwhile, along the S-Ia pathway, the equivalent critical points give endothermic reactions. If the reaction proceeds with **S-o** crossing to the T PSE (given that spin–orbit coupling is presumed to exist between both surfaces in [15]), **T-TSob′** has an activation

Table 3 Total energies (E),[a] zero-point energies (ZPE),[a] imaginary frequencies (ν),[b], spin contamination (S^2), and relative energies (ΔE),[c] of critical points on the singlet ground-state PES in the thermolysis of 3-methyl-1,2,4,5-tetroxane via the S-II pathway. Values for (a) equatorial isomers and (b) axial isomers are shown separately

Structure	E^a	ZPE[a]	ν^b	(S^2)	ΔE^c
(a)					
S-c	−418.51964	0.10414		0.000	0.00
S-TSC	−418.39492	0.09563	831	0.000	72.92
S-P	−418.54087	0.09123		0.072	−21.43
(b)					
S-c	−418.51460	0.10422		0.00	0.00
S-TSC	−418.39393	0.09557	858	0.000	70.29
S-P	−418.49476	0.09111		0.072	4.22

[a] In hartrees

[b] Imaginary frequencies in cm^{-1}

[c] Relative energies in kcal/mol, $\Delta E=[E_{total}+ZPE](c)-[E_{total}+ZPE](i)$ where i represents any critical point of the species in the table

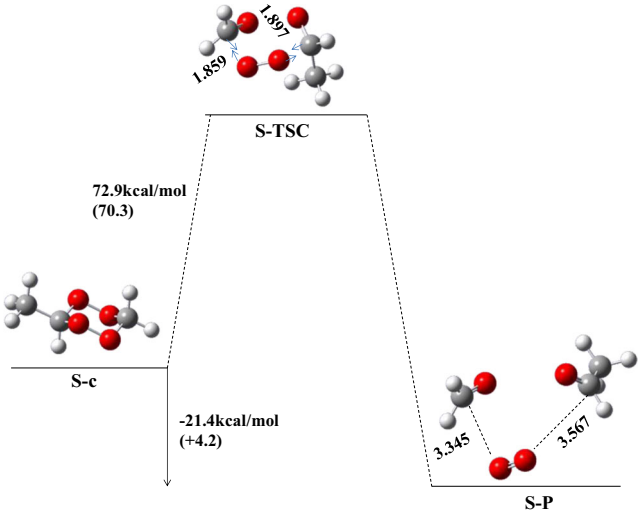

Fig. 5 Reaction profile of pathway S-II in Scheme 1. For each structure, the energies (in kcal/mol) of the equatorial isomer (*not in parentheses*) and the axial isomer (*in parentheses*) are displayed. Bond lengths (in Å) are shown next to the respective bonds. *White, gray, and red spheres* refer to hydrogen, carbon, and oxygen atoms, respectively. The full axial isomer reaction profile is given in the ESM

energy that is higher than the previous steps, so **T-TSob′** can be considered the rate-limiting step of the T stepwise path. However, if surface crossing results in **TSob″** along the the T-Ib pathway, its activation energy is lower than the equivalent in pathway T-Ia, and similar to that of **S-TSco**, where homolytic decomposition of the explosophore bond occurs. In this case, the rate-limiting step of the reaction is unclear because all of the activation energies are very similar. Nonetheless, both pathways clearly result in exothermic reactions.

From **TSbp** in the T-Ia pathway, the reaction proceeds to the product **T-p**, which is found to be 40.1 kcal/mol more stable than **T-b**, with one T oxygen and one acetaldehyde molecule, which is 11.5 kcal/mol more stable than the same structures in the S PES. This complex is more stable than the corresponding S complex because of the greater stability of the T oxygen molecule. This T PES is in good agreement with the known reactivities of peroxide compounds.

Comparison with tetroxane

In pathway T-Ib for the methyl derivative, the reaction evolves from **TSb‴p′** to the product **T-p′**, which is 36.3 kcal/mol more stable than **T-b‴** for both isomers. This comprises one T oxygen and one formaldehyde molecule and shows the same exothermicity as the equivalent reaction in the T-PES of tetroxane; it is also 42.0 kcal/mol more stable than the same structure in the S PES of tetroxane. All reactants and products

Scheme 2 Hypothetical reaction pathways for the T state in the thermolysis of MFDP from the **T-o** diradical intermediate

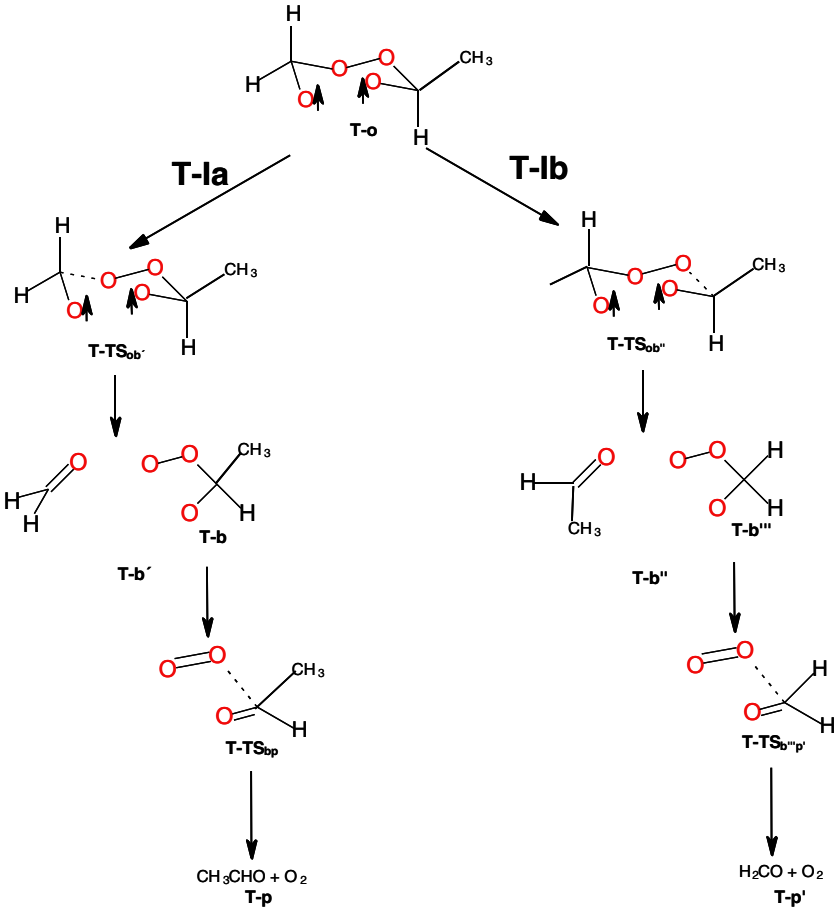

Table 4 Total energies (E),[a] zero-point energies (ZPE),[a] imaginary frequencies (ν),[b], spin contamination (S^2), and relative energies (ΔE),[c] of critical points on the triplet-state PES in the thermolysis of 3-methyl-1,2,4,5-tetroxane via the T-Ia pathway. Values for (a) equatorial isomers and (b) axial isomers are shown separately

Structure	E^a	ZPE[a]	ν^b	(S^2)	ΔE^c
(a)					
T-o	−418.49479	0.09759		2.000	0.00
T-TSob′	−418.45987	0.09546	905	2.000	20.58
T-b′	−418.49904	0.09389		2.000	−4.99
T-b	−304.01987	0.06486		2.000	0.00
T-TSbp	−304.00433	0.06191	3503	2.000	7.90
T-p	−304.08067	0.06172		2.000	−40.12
(b)					
T-o	−418.49317	0.09769		2.000	0.00
T-TSob′	−418.45820	0.09555	894	2.000	20.60
T-b′	−418.49803	0.09378		2.000	−5.50
T-b	−304.01871	0.06506		2.000	0.00
T-TSbp	−304.00356	0.06242	3784	2.000	7.85
T-p	−304.08058	0.06174		2.000	−40.91

[a] In hartrees

[b] Imaginary frequencies in cm^{-1}

[c] Relative energies in kcal/mol $\Delta E=[E_{total}+ZPE](o/b)-[E_{total}+ZPE](i)$ where i represents any critical point of the species in the table

in this reaction step for both tetroxane and its methyl derivative are equivalent. Half of the T-Ia mechanism (where the first reaction product is formaldehyde) is similar for tetroxane and MFDP, with the rate-limiting steps to **T-TSob′** and **S-TSob′** having larger activation energies for tetroxane than MFDP.

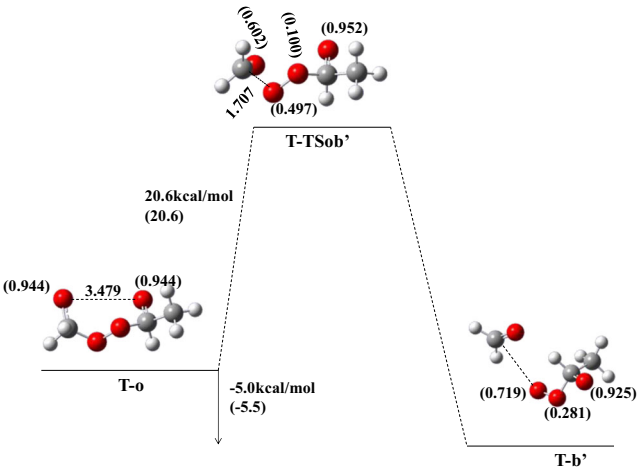

Fig. 6 Reaction profile of the first step of pathway T-Ia in Scheme 2. For each structure, the energies (in kcal/mol) of the equatorial isomer (*not in parentheses*) and the axial isomer (*in parentheses*) are displayed. Activation energies are calculated from **T-o**. Bond lengths (in Å) are shown next to the respective bonds. Spin densities are shown *next to the respective atoms in parentheses*. White, gray, and red spheres indicate hydrogen, carbon, and oxygen atoms, respectively. The full axial isomer reaction profile is given in the ESM

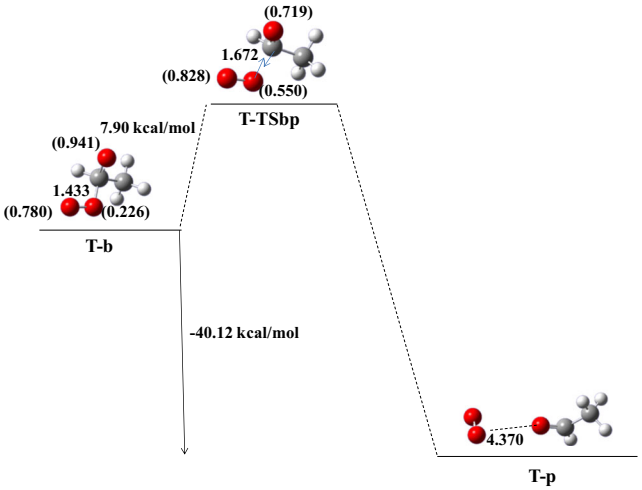

Fig. 7 Reaction profile of the second step of pathway T-Ia in Scheme 2. Activation energies (in kcal/mol) are calculated from T-b. Bond lenghts (in Å) are shown next to the respective bonds. Spin densities are shown *next to the respective atoms in parentheses*

However, the stepwise T-Ib pathway is also similar for tetroxane and MFDP: their respective activation and reaction energies are generally similar, particularly for the step **b‴→ p′**, because of the identities of the intermediate reactant and product.

It is clear that the reaction starts on the S PES, so a crossing point to the T PES would appear to lead to a final T oxygen molecule. In general, the E_{total}+ZPE values of the **T-TS′** species are lower than those of the **S-TS′** species. Therefore, the crossing point should occur between the **o** intermediates because of their similar geometries and stabilities. Besides, for a crossing to occur between PESs with different multiplicities, there should be spin–orbit coupling between the **S-o** and **T-o** structures. Spin–orbit coupling calculations performed at the

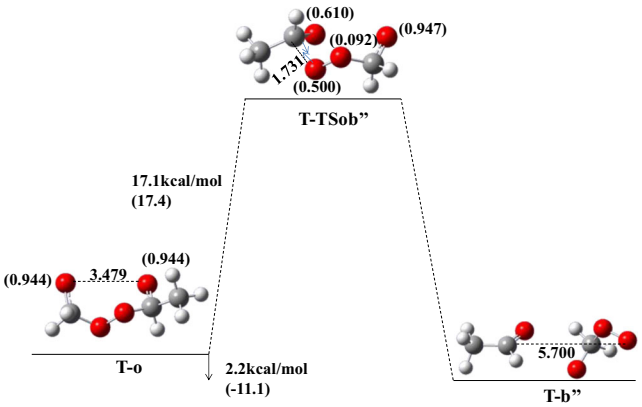

Fig. 8 Reaction profile of the first step of pathway **T-Ib** in Scheme 2. For each structure, the energies (in kcal/mol) of the equatorial isomer (*not in parentheses*) and the axial isomer (*in parentheses*) are displayed. Activation energies are calculated from **T-o**. Activation energies (in kcal/mol) are calculated from **T-o**. Bond lengths (in Å) are shown next to the respective bonds. Spin densities are shown *next to the respective atoms in parentheses White, gray, and red spheres* indicate hydrogen, carbon, and oxygen atoms, respectively. The full axial isomer reaction profile is given in the ESM

Table 5 Total energies (E),[a] zero-point energies (ZPE),[a] imaginary frequencies (ν),[b], spin contamination (S^2), and relative energies (ΔE),[c] of critical points on the triplet-state PES in the thermolysis of 3-methyl-1,2,4,5-tetroxane via the T-Ib pathway. Values for (a) equatorial isomers and (b) axial isomers are shown separately

Structure	E[a]	ZPE[a]	ν[b]	(S^2)	ΔE[c]
(a)					
T-o	−418.49479	0.09759		2.000	0.00
T-TSob″	−418.46411	0.09514	864	2.000	17.15
T-b″	−418.48918	0.09555		2.000	2.24
T-b‴	−264.71349	0.03591		2.000	0.00
T-TSb‴p′	−264.69549	0.03325	3459	2.000	9.63
T-p′	−264.76754	0.03207		2.000	−36.32
(b)					
T-o	−418.49317	0.09769		2.000	0.00
T-TSob”	−418.46311	0.09532	892	2.000	17.37
T-b″	−418.50756	0.09437		2.000	−11.12
T-b‴	−264.71349	0.03591		2.000	0.00
T-TSb‴p′	−264.69549	0.03325	3459	2.000	9.63
T-p′	−264.76754	0.03207		2.000	−36.32

[a] In hartrees

[b] Imaginary frequencies in cm^{-1}

[c] Relative energies in kcal/mol, $\Delta E=[E_{total}+ZPE](o/b)-[E_{total}+ZPE](i)$ where i represents any critical point of the species in the table

CASSCF(10,10)/6- 311+G** level give a value of 74.3 cm^{-1} for both isomers of MFDP, indicating that a nonadiabatic transition can occur from the intermediate **o** on the S PES to the equivalent intermediate on the T PES, with the reaction subsequently proceeding along the T path (Scheme 2). This spin–orbit coupling between both surfaces was also noted for tetroxane; the same value was calculated as for MFDP,

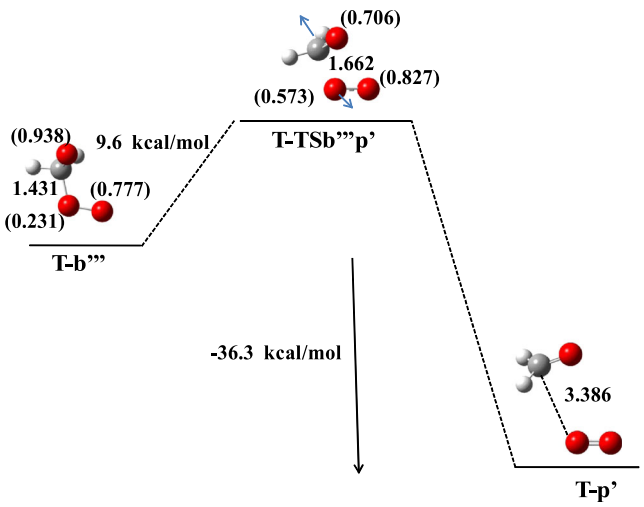

Fig. 9 Reaction profile of the second step of pathway **T-Ib** in Scheme 2. Activation energies (in kcal/mol) are calculated from **T-b‴**. Bond lengths (in Å) are shown next to the respective bonds. Spin densities are shown *next to the respective atoms in parentheses*

indicating that the presence of the methyl substituent does not have any influence on the spin–orbit coupling. However, if the reaction of MFDP proceeds on the T PES from the **o** intermediate, the rate-limiting step is clearly either **TSob′** along the T-Ia pathway (which is found to be 5 kcal/mol, lower than the equivalent step in the tetroxane reaction) or **TSob″** along the T-Ib pathway (here, the activation energy is lower than that for **TSob′**, but equivalent pathway in the tetroxane does not occur.

Upon comparing the energy barriers and exothermicities obtained in the present work for methyltetroxane with those obtained previously for tetroxane [15], it is clear that the former compound should be easier to decompose and should therefore be more reactive and possibly more explosive. It is most interesting to note that this conclusion runs contrary to that drawn on the basis of standard explosivity criteria employed by the energetic materials community. Indeed, it is usually observed that explosive sensitivity is best rationalized in terms of the energy content of the compound and the dissociation energies of so-called explosophore bonds, the homolytic cleavage of which is believed to initiate the decomposition process [42–44]. Accordingly, considering that (1) methyltetroxane exhibits a lower energy content than tetroxane due to its more negative oxygen balance, and (2) methyltetroxane presents a somewhat higher activation energy for O–O homolysis (see [15]), standard sensitivity criteria would predict that methyl tetroxane is less sensitive than tetroxane. Therefore, experimental determination of the decomposition temperatures and/or mechanical sensitivities of both compounds would be extremely valuable. Observation of a lower decomposition temperature and/or a lower drop weight impact height for methyl tetroxane would support the present calculations and demonstrate the need to consider various possible reaction pathways and reaction steps, in some cases involving excited states, when attempting to gauge the stabilities of such compounds.

Conclusions

The thermolysis of MFDP can proceed by at least two stepwise S and T mechanisms, as well as a low-probability concerted S mechanism, all of which yield exothermic products. The first step in the stepwise reactions produces an open diradical intermediate. If the S PES is followed, exothermic products are produced, which contrasts with the endothermic products produced in the equivalent reaction of tetroxane [15]. Spin-orbit coupling occurs between the **o** intermediates on the S PES and the T PES, with the same value observed as for tetroxane. Therefore, a nonadiabatic reaction may be achieved by crossing from the S PES to the T PES, and the reaction then yields one oxygen molecule in its T ground state, one acetaldehyde, and one formaldehyde molecule as products. The greatest exothermicity is attained when the T-Ia pathway is

followed, in which the rate-limiting step is that yielding **TSob′** on both the S PES and the T PES and a formaldehyde molecule is produced. **TSob′/b″** show lower activation energies for MFDP than tetroxane. All of this information suggests that the methyl derivative is more reactive than tetroxane. More investigations should be performed to test the explosive character of each derivative.

Reactant isomers with a methyl group in the equatorial position are more stable than those with an axial methyl. The effect of the conformation of the reactant isomer on the activation energy is more conspicuous when an acetaldehyde molecule is produced in the **o→ b″** step of the S-Ib pathway on the PES.

References

1. Jones CW (1999) Applications of hydrogen peroxides and derivatives. Royal Society of Chemistry, Cambridge
2. Jones CW, Patai S (1983) The chemistry of peroxides. Wiley, New York
3. Ando W (1992) Organic peroxides. Wiley, New York
4. Adam W (2000) Peroxide chemistry: mechanistic and preparative aspects of oxygen transfer. Wiley-VCH, Weinheim
5. Oxley JC, Smith JL, Chen H (2002) Decomposition of a multiperoxidic compound: triacetone triperoxide (TATP). Propellants Explos Pyrotech 27:209–216
6. Vennerstrom JL, Ager AL, Andersen SL, Grace JM, Wongpanich V, Angerhofer CK (2000) Assessment of the antimalarial potential of tetraoxane. Am J Trop Med Hyg 62(5):573–578
7. Li Y, Zhu H, Jiang J, Pan JP, Wu GS, Wu JM, Shi YL, Yang JD, Wu BA (2000) Synthesis and antimalarial activity of artemisinin derivatives containing an amino group. J Med Chem 43:1635–1640
8. Wang X, Dong Y, Wittlin S, Charman SA, Chiu FC, Chollet J, Katneni K, Mannila J, Morizzi J, Ryan E, Scheurer C, Steuten J, Santo Tomas J, Snyder C, Vennerstrom JL (2013) Comparative antimalarial activities and ADME profiles of ozonides (1,2,4-trioxolanes) OZ277, OZ439, and their 1,2-dioxolane, 1,2,4-trioxane, and 1,2,4,5-tetraoxane isosteres. J Med Chem 56(6):2547–2555
9. Kumar N, Singh R, Rawat DS (2012) Tetraoxanes: synthetic and medicinal chemistry perspective. Med Res Rev 32(3):581–610
10. Franco LL, De Almeida MV, Silva LFE, Vieira PP, Pohlit AM, Valle MS (2012) Synthesis and antimalarial activity of dihydroperoxides and tetraoxanes conjugated with bis(benzyl)acetone derivatives. Chem Biol Drug Des 79(5):790–797
11. Leiva LCA, Jorge NL, Romero JM, Cafferata LFR, Gómez Vara ME, Castro EA (2008) Decomposition of the acetone cyclic diperoxide in octanol solution. J Argent Chem Soc 96(1–2):110–122
12. Profeta MI, Romero JM, Leiva LCA, Jorge NL, Gómez Vara ME, Castro EA (2011) Solvent effect of oxygen in the thermolisys decomposition of the acetone diperoxide. Meth Appl Chemoinf Chem Eng 96(1–2):110–122
13. Pila AN, Profeta MI, Romero JM, Jorge NL, Castro EA (2012) Kinetics and mechanism of the thermal decomposition reaction of 3, 6-diphenyl-1,2,3,5-tetroxane in solution. Int J Chem Model 4(4):5–10
14. Reguera MB, Frette SG, Romero JM, Jorge NL, Castro EA (2012) Synthesis and thermical decomposition reaction of 3,6-dibutanoic-1, 2,4,5-tetroxane in solution. Bentham Sci Newsl 4(1):1–4
15. Jorge NL, Romero JM, Grand A, Hernández-Laguna A (2012) Gas-phase thermolysis reaction of formaldehyde diperoxide. Kinetic study and theoretical mechanisms. Chem Phys 39:37–45
16. Reguero M, Bernardi F, Bottoni A, Olivucci M, Robb MA (1991) Chemiluminescent decomposition of 1,2-dioxetanes: an MC-SCF-MP2 study with VB analysis. J Am Chem Soc 113:1566–1572
17. Wilsey S, Bernardi F, Olivucci M, Robb M, Murphy S, Adam W (1999) The thermal decomposition of 1,2-dioxetane revisited. J Phys Chem 103:1669–1677
18. Tanaka S, Tanaka J (2000) Ab initio molecular orbital studies on the chemiluminescence of 1,2-dioxetanes. J Phys Chem A 104(10): 2078–2090
19. Cafferata LFR, Lombardo JD (1994) Kinetic and mechanism of the thermal decomposition reaction of acetone cyclic diperoxide in the gas phase. Int J Chem Kinet 26:503–509
20. Cazut SAI, Ramírez Maisuls EH, Delfino MR, Romero JM, Jorge NL, Castro EA (2009) Thermal decomposition of formaldehyde diperoxide in aqueous solution. Russ J Gen Chem 79(10):2187–2190
21. Leiva LCA, Jorge NL, Romero JM, Cafferata LFR, Gómez Vara ME, Castro EA (2010) Thermal decomposition reaction of 3,3,6,6-tetramethyl- 1,2,4,5-tetroxane in 2-methoxy-ethanol solution. Chem Heterocycl Compd 45(12):1455–1459
22. Leiva LCA, Castellanos GB, Jorge NL, Cafferata LFR, Gómez Vara ME (1998) Kinetics and mechanism of the thermal decomposition reaction of 3,3,6,6-tetramethyl-1,2,4,5-tetroxane in methanol solution. Rev Soc Quím Méx 42(5):223–227
23. Barreto GP, Eyler GN (2011) Thermal decomposition of 3,3,6,6,9,9-hexaethyl-1,2,4,5,7,8-hexaoxacyclononane in solution and its use in methyl methacrylate polymerization. Polym Bull 67(1):1–14
24. Iglesias M, Barreto GP, Eyler GN, Cañizo AI (2010) Thermal decomposition of cyclic organic peroxides in pure solvents and binary solvent mixtures. Int J Chem Kinet 42(6):347–353
25. Becke AD (1988) Density-functional exchange-energy approximation with correct asymptotic behavior. Phys Rev A 38:3098–3100
26. Slater JC (1974) Quantum theory of molecules and solids, the self-consistent field for molecules and solids, vol 4. McGraw-Hill, New York
27. Lee C, Yang LW, Par RG (1988) Development of the Colle–Salvetti conelation energy formula into a functional of the electron density. Phys Rev B 37:785–789
28. Frisch MJ, Trucks GW, Schlegel HB, Scuseria GE, Robb MA, Cheeseman JR, Scalmani G, Barone V, Mennucci B, Petersson GA et al (2004) Gaussian 03, revision C.01. Gaussian Inc., Wallingford
29. Abegg PW, Ha TK (1974) Ab initio calculation of spin-orbit-coupling constant from Gaussian lobe SCF molecular wavefunctions. Mol Phys 27:763–767
30. Abegg PW (1975) Ab initio calculation of spin-orbit-coupling constants for Gaussian lobe and Gaussian-type wave-functions. Mol Phys 30:579–596
31. Flúkiger P, Lúthi HP, Portmann S, Weber J (2000) Gaussview 5.0. Swiss Center for Scientific Computing, Manno
32. Gonzalez C, Schlegel HB (1989) An improved algorithm for reaction path following. J Chem Phys 90:2154–2161
33. Gonzalez C, Schlegel HB (1990) Reaction path following in mass-weighted internal coordinates. J Phys Chem 94:5523–5527
34. Eade RHE, Robb MA (1981) Direct minimization in MC SCF theory: the quasi-Newton method. Chem Phys Lett 83:362–368
35. Siegbahn EM (1984) A new direct CI method for large CI expansions in a small orbital space. Chem Phys Lett 109:417–423
36. Bernardi F, Olivucci M, Robb MA (1990) Mechanism of ground-state-forbidden photochemical pericyclic reactions: evidence for real conical intersections. J Am Chem Soc 112:1737–1744
37. Klene M, Robb MA, Frisch MJ, Celani P (2000) Parallel implementation of the CI-vector evaluation in full CI/CAS-SCF. J Chem Phys 113:5653–5665
38. Koseki S, Gordon MS, Schmidt MW, Matsunaga N (1995) Main-group effective nuclear charges for spin-orbit calculations. J Phys Chem 99:12764–12772

39. Koseki SS, Schmidt MW, Gordon MS (1998) Effective nuclear charges for the first- through third-row transition metal elements in spin-orbit calculations. J Phys Chem 102:10430–10435
40. Leffler JE (1953) Parameters for the description of transition states. Science 117:340–341
41. Hammond GS (1955) A correlation of reaction rate. J Am Chem Soc 77:334–338
42. Mathieu D (2012) Theoretical shock sensitivity index for explosives. J Phys Chem A 116(7):1794–1800
43. Mathieu D (2013) Toward a physically based quantitative modeling of impact sensitivities. J Phys Chem A 117(10):2253–2259
44. Yu Z, Bernstein ER (2013) Sensitivity and performance of azole-based energetic materials. J Phys Chem A 117(42): 10889–10902